

CENTRAL MASS AND LUMINOSITY OF MILKY WAY SATELLITES IN THE Λ CDM MODEL

ANDREA V. MACCIÒ¹, XI KANG¹, BEN MOORE²
The Astrophysical Journal, submitted

ABSTRACT

It has been pointed out that the Galactic satellites all have a common mass around $10^7 M_\odot$ within 300 pc ($M_{0.3}$), while they span almost four order of magnitudes in luminosity (Mateo et al. 1993, Strigari et al. 2008). It is argued that this may reflect a specific scale for galaxy formation or a scale for dark matter clustering. Here we use numerical simulations coupled with a semi-analytic model for galaxy formation, to predict the central mass and luminosity of galactic satellites in the Λ CDM model. We show that this common mass scale can be explained within the Cold Dark Matter scenario when the physics of galaxy formation is taken into account. The narrow range of $M_{0.3}$ comes from the narrow distribution of circular velocities at time of accretion (peaking around 20 km/s) for satellites able to form stars and the not tight correlation between halo concentration and circular velocity. The wide range of satellite luminosities is due to a combination of the mass at time of accretion and the broad distribution of accretion redshifts for a given mass. This causes the satellites baryonic content to be suppressed by photo-ionization to very different extents. Our results favor the argument that the common mass $M_{0.3}$ reflects a specific scale (circular velocity ~ 20 km/s) for star formation.

Subject headings: cosmology: theory — galaxies: dwarf — hydrodynamics — methods: numerical

1. INTRODUCTION

Galaxies are thought to form out of gas which cools and collapses to the center of dark matter haloes (White & Rees 1978). A correlation between stellar mass and host halo mass is thus expected. Observational data, such as from the SDSS, have shown a good correlation between the stellar mass of central galaxies and the halo mass of galaxy groups (e.g. Yang et al. 2007), but such a correlation is not maintained in satellite galaxies (e.g., Gao et al. 2004, Conroy et al. 2007). It is also not clear if such a relation persists to all mass scales. For example, in galaxy clusters, the stellar mass of the central galaxy is not a strong function of the halo mass, because gas cooling and star formation are regulated by the physical processes operating in clusters, such as AGN feedback, which gives rise to a steep luminosity function at the bright end (e.g., Kang et al. 2006).

Mateo et al. (1993) and more recently, Strigari et al. (2008, hereafter S08), claimed that all the satellites with luminosity between 10^3 and $10^7 L_\odot$ to have a common mass of $\sim 10^7 M_\odot$ within a radius of 300pc ($M_{0.3}$), and to be dark matter dominated within this region. This narrow range for central masses compared to the wide range of luminosities has raised the issue if this common mass may reflect a specific scale for galaxy formation or a scale for dark matter clustering.

In this letter, we use a series of high-resolution simulations of MW type haloes combined with a semi-analytical model of galaxy formation to show how this flat relation between $M_{0.3}$ and luminosity arises naturally within our standard cosmological framework combined with simple modelling of the galaxy formation process.

2. SIMULATIONS

Nbody simulations have been carried out using PKDGRAV, a treecode written by Joachim Stadel and Thomas Quinn (Stadel 2001). The cosmological parameters are set in agreement with

the WMAP mission first year results (WMAP1: Spergel et al. 2003) as follows: $\Omega_\Lambda=0.732$, $\Omega_m=0.268$, $\Omega_b=0.044$, $h = 0.71$, $n = 1.0$ and $\sigma_8 = 0.9$. We have selected three candidate haloes with a mass similar to the mass of our Galaxy ($M \sim 10^{12} M_\odot$) from an existing low resolution dark matter simulation (300^3 particles within 90 Mpc) and re-simulated them at higher resolution using the volume renormalization technique (Katz & White 1993). Our high resolution haloes all have a quiet merging history with no major merger after $z = 2$, thus are likely to host a disk galaxy at the present time (as confirmed by our semi-analytic models, see section 3) The high resolution run is 12^3 times better resolved than the low resolution one: the dark matter particle mass is $m_d = 4.16 \times 10^5 h^{-1} M_\odot$, where each dark matter particle has a spline gravitation (comoving) softening of $355 h^{-1}$ pc. Properties of single haloes are listed in Table 1.

For the purpose of constructing accurate merger trees for each simulated galaxy we analyzed 53 outputs between $z = 20$ and $z = 0$. For each snapshot we looked for all virialized haloes within the high resolution region using a spherical overdensity algorithm (see Macciò et al. 2007 for more details on our halo finding procedure). We included in the halo catalogue all haloes with more than 100 particles ($\geq 4 \times 10^7 h^{-1} M_\odot$). For the merger tree construction we started marking all the particles within the 1.5 times the virial radius of a given galaxy at $z = 0$ and we tracked them back to the previous output time. We then make a list of all haloes that at earlier output time containing marked particles, recording the number of marked particles. In addition we record the number of particles that are not in any halo in the previous output time and we consider them as *smoothly* accreted. We used the two criteria suggested in Wechsler et al. (2002) for halo 1 at one output time to be labeled a “progenitor” of halo 2 at the subsequent output time. In our language halo 2 will then be labeled as a “descendant” of halo 1 if i) more than 50% of the particles in halo 1 end up in halo 2 or if ii) more than 75% of halo 1 particles that end up in any halo at time step 2 do end up in halo 2 (this second criterion is mainly relevant during major mergers). A halo can have only one descendant but there is no limit to the number of progenitors. On average there are 20,000 progenitors for each high resolution DM halo.

¹ Max-Planck-Institut für Astronomie, Königstuhl 17, 69117 Heidelberg, Germany; maccio@mpia.de

² Institute for Theoretical Physics, University of Zürich, Winterthurerstrasse 190, CH-8057 Zürich, Switzerland.

3. SEMI ANALYTICAL MODELS

We calculate the luminosity of the satellites using the semi-analytical model for galaxy formation of Kang et al. (2005), and we refer the reader to this paper for more details. Basically we follow the formation history of dark matter haloes and graft the physical models for galaxy formation onto the merger trees. Physical processes governing galaxy formation include: gas cooling from radiative hot gas, star formation and supernova feedback. The original model has been recently updated (Kang 2008) to include photo-ionization to suppress baryon accretion in low mass haloes (Kravtsov et al. 2004), along with a new fitting formula to describe dynamical friction time-scales for satellite galaxies (Jiang et al. 2008). Kang (2008) has shown that this model is successful in reproducing the Milky Way satellite luminosity function and other properties (Macciò et al. in preparation).

There are two important factors which regulate star formation efficiency in low mass dark matter haloes. Firstly, the cooling rate for hot gas in haloes with a virial temperature $T_{\text{vir}} < 10^4 \text{K}$ is quite low due to the inefficiency of H_2 cooling, thus we shut off gas cooling in such haloes. This effect is responsible for the absence of visible satellites with $V_{\text{circ}} \lesssim 16.6 \text{ km/s}$ as shown in Figure 3. Secondly, hot gas accretion is suppressed by the cosmic photo-ionization background in low mass haloes; the typical filtering-mass, at which haloes lose half of their baryonic content, has a strong redshift dependence and it increases from $10^7 M_\odot$ at $z \sim 10$ to $3 \times 10^{10} M_\odot$ at $z = 0$ (Kravtsov et al. 2004). This implies that a satellite galaxy with a halo mass around $10^9 M_\odot$ at infall, has its baryon content suppressed to different extents depending on its accretion redshift. We will see in Section 4 that this gives rise to the wide luminosity range for satellites, despite the narrow range spanned by circular velocities at the accretion time. We set the reionization redshift to be $z_r = 7$ but as shown by Kravtsov et al. (2004) the results of photo-ionization are almost insensitive to the actual value of z_r .

4. RESULTS

The relation between the central mass of a satellite and its circular velocity can be predicted on a theoretical basis, using the well studied relation between mass and concentration. N-body simulations have shown that the spherically averaged density profiles of dark matter haloes can be well described by a two parameter analytic profile (Navarro, Frenk & White 1997, NFW hereafter):

$$\frac{\rho(r)}{\rho_{\text{crit}}} = \frac{\delta_c}{(r/r_s)(1+r/r_s)^2}, \quad (1)$$

where ρ_{crit} is the critical density of the universe, δ_c is the characteristic overdensity of the halo, and r_s is the radius where the logarithmic slope of the halo density profile $d \ln \rho / d \ln r = -2$. A more useful parametrization is in terms of the virial mass,

M_{vir} , and concentration parameter, $c \equiv R_{\text{vir}}/r_s$. The virial mass and radius are related by $M_{\text{vir}} = \Delta_{\text{vir}} \rho_{\text{crit}} (4\pi/3) R_{\text{vir}}^3$, where Δ_{vir} is the density contrast of the halo. Then the mass within 300 pc is simply defined by:

$$M_{0.3} = \int_0^{r_{0.3}} 2\pi t^2 \rho(t) dt = 4\pi \rho_{\text{crit}} \delta_c r_s^3 \left(\log(1+x) - \frac{x}{1+x} \right) \quad (2)$$

where $x \equiv r_{0.3}/r_s$ and the value of $M_{0.3}$ only depends on the two parameters defining the density profile: r_s (or the concentration c) and δ_c . Several models have been proposed to link mass and concentration of dark matter haloes (Bullock et al. 2001, Eke et al. 2001, Macciò et al. 2007), recently Macciò et al. 2008 have proposed a new toy model (based on a modification of original model of Bullock et al. 2001) to predict the concentration mass relation in dark matter haloes. Using this model it is then possible to predict the value of $M_{0.3}$ as a function of the circular velocity of the halo.

Figure 1 shows the values for the mass within 300 pc in the WMAP5 cosmology (Komatsu et al. 2008) as a function of the circular velocity of the dark matter halo. Dashed lines represent the one σ scatter as expected from Nbody simulations (here we use a constant value of 0.1 dex Macciò et al. 2008). The dotted horizontal lines show the mass range observed for Milky Way satellites (S08). The range of circular velocities that is in agreement with observational data (shaded gray region in the figure) is fairly large and covers almost the entire range of plausible values for V_{circ} .

There are two possible issues with this kind of approach: firstly, we are extrapolating to lower masses a relation (c/M) that has been tested on N-body simulation only down to a mass of $\sim 10^{10} M_\odot$, well above the expected masses for Milky Way

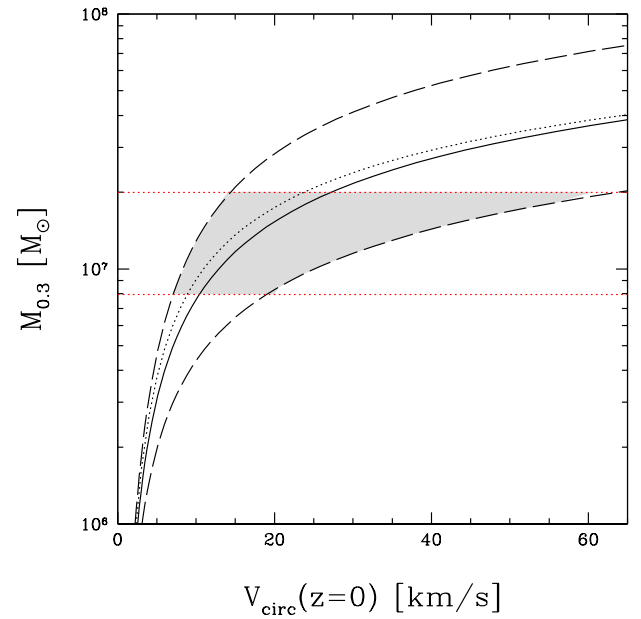


FIG. 1.— Theoretical prediction of the mass within 300 pc versus circular velocity using the toy model of Macciò et al. 2008 for the mass concentration relation: solid line and dashed lines represent the median and two σ scatter respectively for the WMAP5 model (the dotted line shows the median for the WMAP1 model). The dotted (red) horizontal lines show the mass range observed Milky Way satellites (S08). The shaded region gives a visual impression of circular velocities for which the values of $M_{0.3}$ consistent with observations are expected.

TABLE 1
GALAXIES PARAMETERS

Halo	Mass ($10^{12} h^{-1} M_\odot$)	Npart	R_{vir} (kpc/h)	MaxVcirc (km/s)
G0	0.88	2115385	197	179.6
G1	1.22	2931295	219	187.6
G2	1.30	3123511	250	203.1

satellites. Secondly, satellites we see today can be a biased sample of the overall dark matter halo population since they are the surviving population which possibly form prior to reionisation (Moore et al. 2006). For these reasons a full numerical inspection of origin of the narrow range for $M_{0.3}$ is needed.

In order to compare numerical results to observations, for each simulated satellite we need both its luminosity L and its inner mass $M_{0.3}$. The first quantity is a direct outcome of our semi-analytical model, whilst to compute the second quantity we proceeded in the following way: at time of accretion of each satellite we compute the density profile directly from its particle distribution in the N-body simulation. The resulting numerical density profile is then fitted with an NFW profile (Eq. 1); during the fitting procedure we treat both r_s and δ_c as free parameters. Their values, and associated uncertainties, are obtained via a χ^2 minimization procedure (see Macciò et al. 2008 for more details). We are only interested in dark matter haloes that host a galaxy according to our semi-analytic model; given that gas cooling is allowed only in haloes with $M \gtrsim 10^8 h^{-1} M_\odot$ (i.e. $T_{\text{vir}} > 10^4 \text{K}$) this implies that, on average, we have more than 1,000 particles per halo at time of accretion, which is sufficient to obtain a robust estimation of the density profile parameters (Macciò et al. 2007). Under the assumption that the density profile within 300 pc does not evolve from the time of accretion to $z = 0$ we can compute, for each satellite, the present value of $M_{0.3}$ using equation 2.

The upper panel in Figure 2 shows the results for the relation between the mass within 300 pc and luminosity as obtained in our numerical model (red dots) versus the observational results (black dots with error bars). Here we plot results only for simulated satellites that satisfy the detection threshold of the SDSS as determined by Koposov et al. 2007. This means that the satellite luminosity and distance have to satisfy the following relation $\log(R/\text{kpc}) < 1.04 - 0.228 M_v$. The mean and the

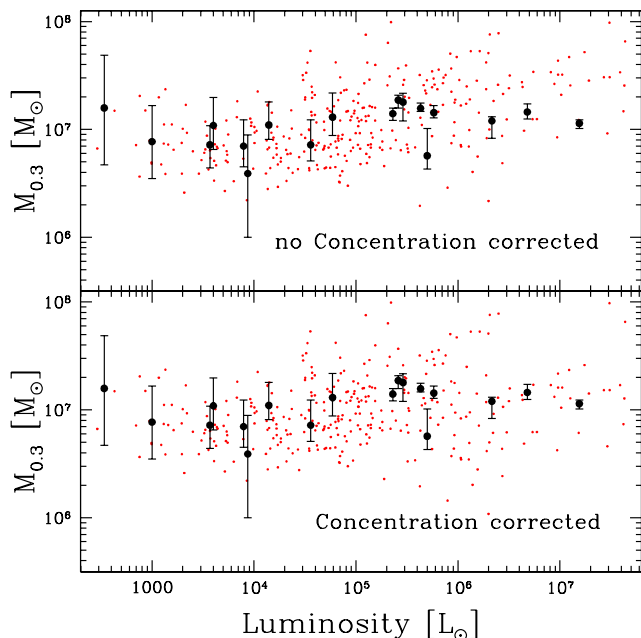


FIG. 2.— Mass within 300 pc versus luminosity. Red dots show results from our numerical model, black points with error bars are the observational results from S08. Upper panel: no correction for the concentration related density evolution. Lower panel: correction included (see text).

scatter of observational data are both well reproduced by our numerical results up to a luminosity of $L = 2 \times 10^6 L_\odot$, after this point simulations seem to suggest an increase with luminosity of $M_{0.3}$, which is not present in the data (even if only three satellite galaxies have a luminosity greater than $10^6 L_\odot$).

These results are obtained under the assumption of no evolution for the parameters defining the density profile (r_s and δ_c). This assumption is motivated by the detailed numerical study carried out by Kazantzidis et al. 2004 (K04, hereafter, see also the recent results by and Peñarrubia et al. 2008). K04 have shown that the inner density profile is extremely robust and that it is unmodified by tidal forces even after tidal stripping removes a large fraction of the initial mass. They have also shown that the degree of modification (if any) of the density profile depends on the initial (i.e. before infall) concentration of the satellite dark matter halo. While highly concentrated haloes (with $c \gtrsim 15$) are able to keep the profile unchanged even after several orbital periods, less concentrated haloes ($c \approx 9$) slightly modify their profile mainly by reducing the overall normalization (δ_c) by approximately a factor 2 (see also Mayer et al. 2006).

In order to take into account this expected modification of the density profile in low concentration haloes, we manually reduce the δ_c parameter by a factor 2 in all haloes with concentration less than 10 at the moment of infalling. In doing this correction we used the value of the concentration extrapolated to $z=0$, in other words we multiplied the value of the concentration at z_{acc} by $(1+z_{\text{acc}})$ in order to take into account the redshift evolution of R_{vir} . Results are shown in lower panel of Figure 2. As expected this modification mainly applies to high luminosity haloes, since they were the most massive ones at time of infall, and thus likely to be less concentrated (the average concentration of our haloes is 16.3 ± 7.1 , and 74% have $c > 10$). When a possible modification of the density profile for low concentration haloes is taken into account the up turn in the numerical $M_{0.3}/L$ relation at high luminosities almost vanishes and numerical results are now in better agreement with the observational data. There are still some haloes with $M_{0.3} > 3 \times 10^7$ around $L = 10^6$, these haloes formed at high redshift, and thus happen, by chance, to have a high c (i.e. they are not affected by our correction) and a large L ; besides of that they do not present any other peculiar behavior.

The presence of a baryonic component inside the dark matter halo can by itself modify the density profile of the halo, due to the adiabatic compression process (e.g. Blumenthal et al. 1986). In our case we expect this effect to be negligible given that the baryon fraction of our haloes is much lower than the universal one and satellites have been observed to be dark matter dominated even in their central regions (S08).

Now we turn to understand the origin of the relation between $M_{0.3}$ and L found by S08. In upper panel of Figure 3 we show the distribution of V_{circ} at the time of accretion for visible satellites (same sample used in Figure 2). The distribution peaks around $V_{\text{circ}} = 20$ km/s and then declines sharply towards higher values of the circular velocity. As discussed in Section 3, the sharp cutoff below $V_{\text{circ}} \sim 20$ km/s comes from the shut off of cooling in haloes with virial temperature below 10^4K . Combining this narrow distribution of circular velocity (between 20–40 km/s) with the theoretical expectations shown in Figure 1, and assuming that $M_{0.3}$ does not evolve after accretion, it is not surprising that all Milky Way satellites (observed and simulated) have a inner mass within 300 pc always around $10^7 M_\odot$. It is then interesting to ask why these satellites span a wide range

of luminosity. In the lower panel of Figure 3, we show the dark matter mass of satellites at their time of accretion, and the dashed line shows the evolution of the filter mass, defined as the mass of a halo in which half of its baryons have been lost due to photo-ionization. We can see that most satellites have mass lower than the filter mass at accretion, and at a given accretion mass, there is wide range of accretion redshifts, which give rise to different amounts of baryon suppression. The spread in Luminosity originates then from the range of halo masses at time of accretion combined with the large scatter (at a given mass) in the accretion time.

Recently Okamoto, Gao & Theuns (2008) have shown that the actual values of the filter mass might be smaller than what suggested by Kravtsov et al. (2004). The effect of a lower filtering mass will be to increase the satellite luminosity for a given V_{circ} ; this will push all points in Figure 2 towards the right; but will not alter the flat relation between $10^4 L_{\odot}$ and $10^7 M_{\odot}$.

Whilst this paper was ready for submission a similar study was posted on the arXiv (Li et al. 2008). These authors used a similar approach (an Nbody simulation combined with a semi-analytic model for galaxy formation) to study the relation between central mass and luminosity in (satellite) dwarf galaxies. The main difference with respect to this work is that Li et al. (2008) computed the inner mass of satellites directly from the Nbody simulation. Given the spatial resolution of their simulation (0.18 kpc) they presented results for $M_{0.6}$ (mass within 600 kpc) which turned out to be in excellent agreement with observational data of Strigari et al. (2007). This study is complementary to ours.

5. SUMMARY AND CONCLUSIONS

The observational evidence that all Milky Way satellites have a common mass of about $10^7 M_{\odot}$ within their central 300 parsecs has raised issues about the possible existence of a new

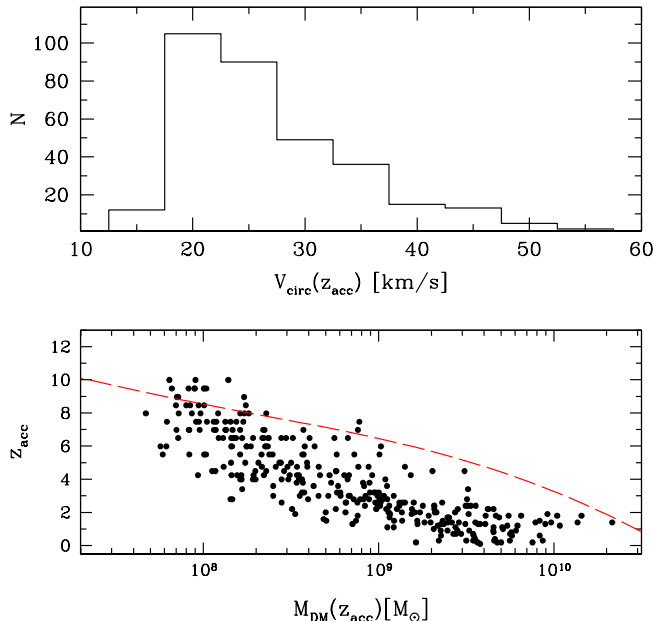


FIG. 3.— Upper panel: distribution of the circular velocities at the time of accretion for visible satellites. Lower panel: accretion redshift vs satellite halo mass at accretion time. The (red) dashed line shows the redshift evolution of the filtering mass for UV photoionization.

scale in galaxy formation or a characteristic scale for the clustering of dark matter. In this Letter, by using high resolution numerical simulations combined with a semi analytic model for galaxy formation, we show that this common mass scale can be easily explained within the current (Λ)CDM model for structure formation.

The observational data on the $L/M_{0.3}$ relation can be successfully reproduced in numerical simulations, up to a luminosity of $10^6 L_{\odot}$ under the assumption that the parameters describing the density profile of satellite galaxies do not evolve significantly after these galaxies have been accreted into the main halo. When a plausible (small) modification of such parameters, for low concentration haloes, is taken into account, the agreement with observational data extends to the whole luminosity range.

According to our numerical modeling this common mass scale, $M_{0.3} \sim 10^7 M_{\odot}$, originates from the narrow range of circular velocities (20-40 km/s) spanned by visible satellites at the time of accretion (with a lower limit of 17 km/s set by the inefficiency of H_2 cooling in halo with virial temperature below 10^4 K). On the other hand the wide range of luminosities comes from the range of halo masses at time of accretion combined with the large scatter in the accretion time for an halo with a given mass, which has a strong impact on the ability of photo reionization of reducing the baryon content of satellites, and thus determining their luminosity.

Our results show that the observed flat relation between satellite inner mass and luminosity can be easily explained within the CDM framework, without modifying the nature of dark matter particles.

The authors thank L. Strigari for making his results publicly available. Frank van den Bosch and Sergey Koposov are gratefully acknowledged for interesting discussions and useful comments. An anonymous referee is also thanked for his/her comments that improved the presentation of this paper. Numerical simulations were performed on the PIA cluster of the Max-Planck-Institut für Astronomie at the Rechenzentrum in Garching.

REFERENCES

- Blumenthal, G. R., Faber, S. M., Flores, R., & Primack, J. R. 1986, ApJ, 301, 27
- Bullock, J. S., Kolatt, T. S., Sigad, Y., Somerville, R. S., Kravtsov, A. V., Klypin, A. A., Primack, J. R., & Dekel, A. 2001, MNRAS, 321, 559 (B01)
- Conroy, C., Wechsler, R.H., & Kravtsov, A.V., 2007, ApJ, 668, 826
- Eke, V. R., Navarro, J. F., & Steinmetz, M. 2001, ApJ, 554, 114
- Gao, L., De Lucia, G., White, S. D. M., & Jenkins, A., 2004, MNRAS, 352, 1
- Jiang, C.Y., Jing, Y.P., Faltenbacher, A., Lin, W.P., & Li, C., 2008, ApJ, 675, 1095
- Kang, X., Jing, Y.P., Mo, H.J., Börner, G., 2005, ApJ, 631, 21
- Kang, X., Jing, Y.P., Silk, J., 2006, ApJ, 648, 820
- Kang, X., 2008, Proceedings of IAU 254 "The Galaxy Disk in Cosmological Context", arXiv:0806.3279
- Katz, N., & White, S. D. M. 1993, ApJ, 412, 455
- Kazantzidis, S., Mayer, L., Mastrogiro, C., Diemand, J., Stadel, J., & Moore, B. 2004, ApJ, 608, 663
- Komatsu, E., et al. 2008, arXiv:0803.0547
- Koposov, S., et al. 2008, ApJ, 686, 279
- Kravtsov, A.V., Gnedin, O.Y., & Klypin, A.A., 2004, ApJ, 609, 482
- Li, Y.-S., Helmi, A., De Lucia, G., & Stoehr, F. 2008, arXiv:0810.1297
- Macciò, A. V., Dutton, A. A., van den Bosch, F. C., Moore, B., Potter, D., & Stadel, J. 2007, MNRAS, 378, 55
- Macciò, A. V., Dutton, A. A., van den Bosch, F. C., 2008, MNRAS in press, arXiv:0805.1926
- Mayer, L., Mastrogiro, C., Wadsley, J., Stadel, J., & Moore, B. 2006, MNRAS, 369, 1021

- Mateo, M., Olszewski, E. W., Pryor, C., Welch, D. L., & Fischer, P. 1993, *AJ*, 105, 510
- Moore, B., Diemand, J., Madau, P., Zemp, M. & Stadel, J. 2006, *MNRAS*, 368, 563
- Navarro, J. F., Frenk, C. S., & White, S. D. M. 1997, *ApJ*, 490, 493
- Okamoto, T., Gao, L., & Theuns, T., 2008, *MNRAS*, 390, 920
- Peñarrubia, J., Navarro, J. F., & McConnachie, A. W. 2008, *ApJ*, 673, 226
- Spergel, D. N., et al. 2003, *ApJS*, 148, 175
- Stadel, J. G. 2001, Ph.D. Thesis, University of Washington
- Strigari, L. E., Bullock, J. S., Kaplinghat, M., Diemand, J., Kuhlen, M., & Madau, P. 2007, *ApJ*, 669, 676
- Strigari, L. E., Bullock, J. S., Kaplinghat, M., Simon, J. D., Geha, M., Willman, B., & Walker, M. G. 2008, *Nature*, 454, 1096, (S08)
- Wechsler, R. H., Bullock, J. S., Primack, J. R., Kravtsov, A. V., & Dekel, A. 2002, *ApJ*, 568, 52
- White, S. D. M., & Rees, M. J. 1978, *MNRAS*, 183, 341
- Yang, X.H., Mo, H.J., Van den Bosch, F.C., Pasquali, A., Li, C., & Barden, M., 2007, *ApJ*, 671, 153